Mapping of Two "Neutralizing" Epitopes of a Snake Curaremimetic Toxin by Proton Nuclear Magnetic Resonance Spectroscopy

Sophie Zinn-Justin, Christian Roumestand, Pascal Drevet, André Ménez, and Flavio Toma*

Département d'Ingénierie et d'Etude des Protéines, CE-Saclay, 91191 Gif-sur-Yvette Cedex, France

Received December 28, 1992; Revised Manuscript Received April 1, 1993

ABSTRACT: Two monoclonal antibodies, called Mα1 and Mα2,3, have been previously shown to neutralize the toxic activity of the curaremimetic toxin α from *Naja nigricollis*. In this paper, we report the mapping of the two corresponding epitopes, using affinity chromatography and proton 2D-NMR spectroscopy. The H–D exchange rates of labile amide hydrogens have been measured in toxin α bound to each antibody and in toxin α alone. Analysis of the exchange data revealed two regions containing amide hydrogens with decreased exchange rates in the bound toxin compared to the free toxin. These two regions correspond to the sites of interaction with Mα1 and Mα2,3, respectively. They are consistent with prior biochemical mapping studies, and they include several residues that were not previously identified. Thus, the two antigenic sites are found to be centered on two different loops of toxin α. Comparison of these antigenic sites with the active site of toxin α allows us to delineate the molecular events associated with the two neutralization processes.

The sites by which proteins interact with antibodies play a critical role in the protection process of the immune response and are therefore currently the subject of extensive studies. The complete three-dimensional description of epitopes has been achieved in a few cases by X-ray diffraction [for reviews, see Davies et al. (1990) and Tulip et al. (1992)]. Thus, it has been shown that epitopes are constituted of about 15 residues located in several discrete segments of the polypeptide chain; the segments form a contiguous interaction surface as a result of the folding of the protein. This topographical property of epitopes makes their identification difficult and hence limits the number of mapping methods. Several approaches have been developed which avoid going through crystallization of the antibody–antigen complex. However, these methods only provide a partial view of the antigenic site. They include the use of panels of evolutionarily related proteins to identify immunodominant residues (Urbanski & Margoliash, 1977; Jemmerson & Margoliash, 1979; Benjamin et al., 1984), analysis of the immunoprotection of antigenic residues against chemical modification (Burnens et al., 1987) or proteolysis (Jemmerson & Paterson, 1986a,b), and mapping with synthetic peptides (Benjamin et al., 1984; Berzofsky, 1985; Jemmerson & Paterson, 1986a,b). Chemical modifications (Jemmerson & Margoliash, 1979, 1981; Boulain et al., 1982; Trémeau et al., 1986; Cooper et al., 1987; Collawn et al., 1988) and site-directed mutagenesis of the protein antigen (Pillet, 1991) have also been used to identify residues involved in the antibody–antigen interactions.

Recently, it has been shown that proton 2D-NMR[1] provides a means for the mapping of protein epitopes (Paterson et al., 1990; Paterson, 1992; Mayne et al., 1992). The principle of the method, which has also been used to study other protein–protein complexes (Brandt & Woodward, 1987; Werner & Wemmer, 1992), is the following. Exchange behavior can be observed by NMR for a substantial proportion of individual amide and labile side-chain hydrogens; the effect of antibody binding is characterized by comparing the exchange rates measured on the free protein and on the protein bound to the antibody: the protons that become protected against exchange by antibody shielding define the binding region of the antibody in the protein (Paterson et al., 1990).

The purpose of the present work is to determine and compare by this approach the interaction sites of a curaremimetic toxin with two neutralizing antibodies. The antigen, toxin α from *Naja nigricollis* venom (Eaker & Porath, 1967), is a structurally well-characterized protein (Zinn-Justin et al., 1992), which binds specifically and with high affinity to the nicotinic acetylcholine receptor, thus blocking the nerve–muscle transmission. The two neutralizing antibodies, called Mα1 and Mα2,3, inhibit the binding of toxin α to the nicotinic acetylcholine receptor (Boulain et al., 1982; Trémeau et al., 1986). They seem to act in different ways, since Mα1 accelerates the dissociation of the toxin α-receptor complex (Boulain & Ménez, 1982), whereas Mα2,3 has no such effect on the dissociation rate of the complex (our unpublished data). Understanding of the molecular events that are associated with the neutralization processes requires the comparison and hence the delineation of both the toxic site and the epitopes recognized by Mα1 and Mα2,3. Previous attempts in this respect have been made by measuring the receptor binding affinity of various toxin α analogs, including chemically modified derivatives of toxin α [reviewed in Endo and Tamiya (1987, 1991)] and site-directed mutants of the highly homologous curaremimetic erabutoxin a (Pillet et al., 1993). Thus, it has been shown that the curaremimetic site essentially involves residues in loops 2 and 3 of short-chain curaremimetic toxins. Conversely, only a few residues of the Mα1 or Mα2,3 epitopes have been identified (Boulain et al., 1982; Trémeau et al., 1986); therefore, additional evidence is required for the complete characterization of the antigenic sites.

In this paper, we show that the interaction of toxin α with the Mα1 and Mα2,3 antibodies affects the amide exchange behavior in two topographically distinct regions of the toxin. From these NMR data and the previous biochemical results, the two binding sites are described. Finally, the corresponding neutralization processes are discussed.

* To whom correspondence should be addressed.

[1] Abbreviations: NMR, nuclear magnetic resonance; 2D, two-dimensional; COSY, correlated spectroscopy.

0006-2960/93/0432-6884$04.00/0 © 1993 American Chemical Society

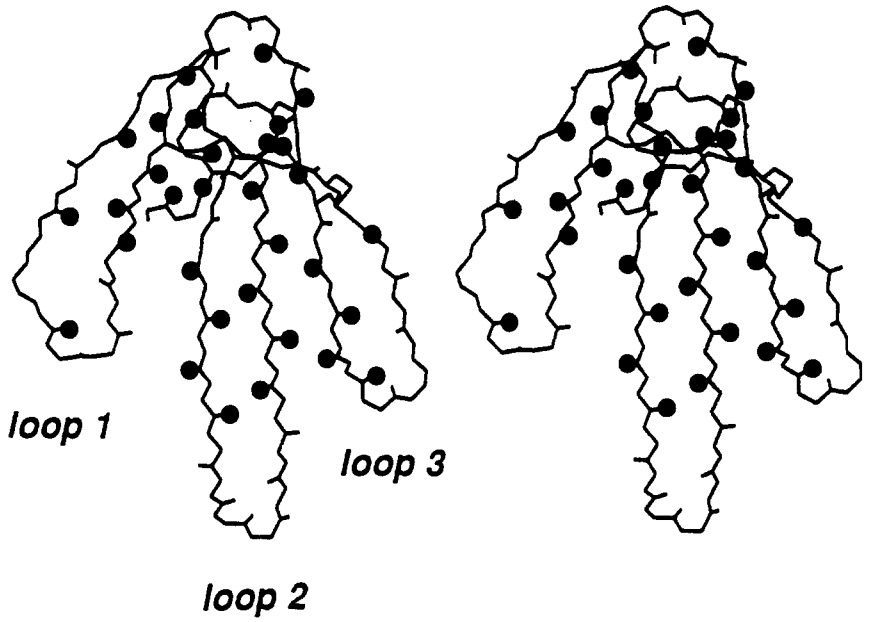

FIGURE 1: Stereoview of the average backbone structure of toxin α (Zinn-Justin et al., 1992). The black spheres represent the amides of toxin α whose exchange kinetics can be followed in the complex by the indirect method, provided that these amides do not fully exchange in the complex before the recording of the first spectrum. They correspond to protons which do not fully exchange between the end of the exchange time in the complex and the beginning of the recording of the NMR signal, i.e., to protons with a kinetic constant (k_{obs}) lower than 1/60 min^{-1} at pH 3.5 and 283 K.

MATERIALS AND METHODS

Materials

Toxin α was purified from *Naja nigricollis* venom (Institut Pasteur, Paris, France) as previously published (Fryklund & Eaker, 1975). Preparation of the monoclonal antibodies Mα1 and Mα2,3 (IgG2a subclass) has been described by Boulain et al. (1982) and by Trémeau et al. (1986), respectively. The immunization was achieved by injecting increasing doses of toxin α into mice. The fusion procedure was carried out according to Köhler and Milstein (1975). The resulting monoclonal hybridoma cells which produced antitoxin α were grown intraperitoneally in mice. Antibodies were purified from ascitic fluids by affinity chromatography on a toxin α–Sepharose column.

Deuterium oxide, DCl, NaOD, and deuteriated acetic acid were from CEA (99.98 atom % D). Fifty millimolar K_2D/KD_2PO_4, pH 7.4, was obtained by dissolving the salt in D_2O, lyophilizing the solution, redissolving the salt in D_2O, and adjusting the pH to 7.4 with microliter amounts of dilute DCl or NaOD. The pH of deuteriated solutions was measured without correction of the isotopic effect.

Methods

Hydrogen Exchange of Free Toxin α. Proton–deuterium exchange of amide groups was studied on a 7 mM sample of toxin α lyophilized from H_2O and redissolved in D_2O, pH 3.5. The exchange kinetics of the individual protons was followed with time at 283 K by 2D-NMR absolute-value COSY experiments (Aue et al., 1976; Nagayama et al., 1980) recorded on a Bruker AMX600 spectrometer. Each experiment consisted of eight scans of 1024 complex data points covering a spectral width of 7812.5 Hz for 256 t_1 increments. Total acquisition time was 25 min, so that spectra could be recorded every 30 min during 24 h. Exchange rates (k_{obs}) were determined by a least-squares fit of the exponential decay of the ($NH,C^{\alpha}H$) peak volumes as a function of time.

The same method was applied to calculate proton–deuterium exchange rates (k_{free}) on a sample of toxin α redissolved in 50 mM K_2D/KD_2PO_4, pH 7.4, at 283 K.

Hydrogen Exchange of Antibody-Bound Toxin α. One hundred milligrams of monoclonal antibody was coupled to 20 mL of Hydrazide Avidgel (Interchim); the Hydrazide Avidgel allowed oriented Fc region specific attachment of antibodies to the gel phase. Eight milligrams of toxin α was loaded onto the antibody column. Unbound toxin was removed by copiously washing the column with potassium phosphate buffer (50 mM KH_2/K_2HPO_4 at pH 7.4). About 7 mg of antigen remained fixed to the antibodies.

In order to initiate exchange, the column was rapidly washed (1 mL/min) with 3 dead volumes of 50 mM KD_2/K_2DPO_4 at pH 7.4 and was incubated at 283 K during periods of time ranging from 1 to 24 h. Ten minutes before the end of the incubation, the column was washed with a low-capacity buffer (1 mM KD_2/K_2DPO_4 at pH 7.4). The toxin was then eluted in about 10 mL of 0.2 M acetic acid at pH 2.5 and 277 K and was immediately lyophilized. The fraction was redissolved in 1 mL of D_2O, its pH was eventually readjusted to 3.5 with microliter amounts of DCl or NaOD, and the fraction was again immediately lyophilized. The procedure was repeated for seven different exchange times: 1, 2, 3, 5, 8, 16, and 24 h. The same column was used for the seven experiments.

Finally, each sample was analyzed by 2D-NMR spectroscopy: the fraction was redissolved in D_2O, and an absolute value COSY spectrum was immediately recorded at 283 K on the Bruker AMX600 spectrometer. The experiment consisted of 64 scans of 1024 complex data points covering a spectral width of 7812.5 Hz for 256 t_1 increments. Total acquisition time was 4 h, 11 min.

Peak volumes were measured for the resolved ($NH,C^{\alpha}H$) cross peaks, and the exchange rates (k_{bound}) were determined from their exponential decay as a function of the H–D exchange time. A protection factor, $\tau = k_{free}/k_{bound}$, was finally calculated for each amide in both complexes.

RESULTS

Frame of the Study. As shown by the previous 2D-NMR study of toxin α (Zinn-Justin et al., 1992), the ($NH,C^{\alpha}H$) cross peaks corresponding to most amide protons are well

separated; therefore, the individual exchange kinetics could be followed in free toxin α by recording the 2D-NMR spectra directly and continuously while exchange was in progress. Since the first NMR experiment was started a few minutes after the toxin was dissolved in D_2O, the kinetic constants of relatively fast exchanging protons (i.e., $1/k > 15$ min) could be measured. The same experiments were not feasible directly on the antibody–toxin complex. Therefore, an indirect approach was used to study the exchange in the toxin bound to the antibody: after exchange had occurred in the complex at pH 7.4 for different periods of time, spectra corresponding to the different exchange times were recorded on toxin α alone at low pH in order to minimize further exchange. The two approaches have been shown to yield comparable kinetic constants (Werner & Wemmer, 1992). However, the indirect method does not allow the observation of protons that fully exchange during the time period corresponding to the elution of the toxin from the complex and the preparation of the NMR sample. Thus, in this method, the observable protons are limited to those of the amides that are not fully exchanged after 1 h at pH 3.5 and 283 K.

Analysis of the exchange data at pH 3.5 and 283 K showed that 32 amides have a kinetic constant (k_{obs}) such that $1/k_{obs} > 60$ min. As illustrated in Figure 1, the 32 amides are widely distributed throughout the whole toxin; thus, information on the epitopes is potentially accessible in the entire structure. More precisely, eight of these amides are in loop 1, fourteen are in loop 2, five are in loop 3, and five are in the C-terminal part of the molecule. They are predominantly found in the β-sheet regions of the toxin and are rarely found at positions i, $i + 1$, and $i + 2$ of turns, i.e., at the tips of the loops of the toxin. It must be stressed that none are found at the tip of loop 2. In the following, we will only refer to these 32 amides which can be observed by the indirect method.

Exchange Measurements in the Free Toxin. The H–D exchange rates in free toxin α have been measured at pH 7.4 and 283 K, in order to further compare them to the exchange rates measured under the same conditions in the toxin bound to the antibody. Among the 32 potentially observable amides, 19 are still observable after 15 min of exchange at pH 7.4 and 283 K. However, exchange rates could be measured only for 12 of them (Table I). The seven remaining amides, corresponding to C3, H4, C23, Y24, K26, E37, and C54, are totally unexchanged during the longest incubation time: obviously, they do not constitute appropriate probes for the investigation of a H–D exchange slowing associated with complex formation. Only an increase of their exchange rates might be observed upon complex formation and thus might provide structural and dynamics information on the complex.

Exchange Measurements in the Antibody–Toxin Complexes. Figure 2 presents COSY spectra of toxin α recorded after incubation with Mα1 and Mα2,3 over two different times. Each spectrum shows numerous cross peaks that are not observed in the spectrum of the free toxin recorded at the same exchange time. These additional peaks result from antibody binding. They correspond to different residues according to the antibody which binds toxin α. The curves in Figure 3 illustrate more quantitatively the difference of exchange behavior between the amides in the Mα1-bound toxin and the amides in the Mα2,3-bound toxin. Thus, the exchange of the amide of N5 is slowed when the toxin binds to Mα1, whereas it is not affected when the toxin binds to Mα2,3. In contrast, the amide of R38 exchanges more slowly when the toxin is bound to Mα2,3 compared to the toxin in the free state or when bound to Mα1.

Table I: H–D Exchange Rates of the Amide Protons in Free Toxin α (k_{free}), in Toxin α Bound to Mα1 (k_1), and in Toxin α Bound to Mα2,3 ($k_{2,3}$)[a]

residue	$1/k_{free}$ (min)	$1/k_{2,3}$ (min)	$\tau_{2,3}$	$1/k_1$ (min)	τ_1
N5	110	120	1	>10 000	>92
Q6	30	4300	143	<60	<2
T13	140	1110	8	6490	46
K15	100	3060	31	>10 000	>100
K25	200	3060	15	1120	6
V27	50	1540	31	60	1
W28	2980	>10 000	>3	7550	3
I35[b]	<15	1460	>97	70	>5
I36[b]	<15	530	>35	70	>5
R38	30	1740	58	70	2
G41[b]	<15	110	>7	<15	
N52[b]	<15	30	>2	<15	
T56	100	210	2	260	3
K58	30	280	9	1730	58
C59	30	4140	138	<60	<2
N60	110	100	1	460	4

[a] Residues with measurable kinetic constants under the exchange conditions (pH 7.4, 283 K) are listed. Their protection factors τ_1 and $\tau_{2,3}$ are calculated in the two complexes. Seven amides remained unexchanged after 24 h in the free and the bound toxin; they correspond to residues C3, H4, C23, Y24, K26, E37, and C54. The other amides exchange too fast to be observable in the free and the bound toxin. [b] Amide protons totally exchanged in less than 15 min in the free toxin.

The data in Figure 3 also illustrate the quality of the H–D exchange data generally obtained. The exponential fit obtained for all the curves corresponds to an average correlation coefficient of 0.953 (root mean square, 0.062; allowable error, 0.01%). The errors on the values of the exchange rates essentially depend on the signal/noise ratio corresponding to the NMR spectra. In order to take into account these errors, only protection factors larger than 10 were considered for assigning protected amides.

Twenty three out of the 32 potentially observable amides are still observable in at least one complex after 1 h of exchange at pH 7.4 and 283 K. Seven of these amides, corresponding to C3, H4, C23, Y24, K26, E37, and C54, are totally unexchanged after the longest incubation time in both complexes. They were already found to be unexchanged under the same conditions in the free toxin, and therefore no protection factor could be calculated for them. Table I summarizes the results found for the 16 remaining amides. Antibody binding dramatically reduces the H–D exchange rates of some amides, with protection factors larger than 100.

H–D Exchange in Mα1-Bound Toxin. The amides of N5 and K15, which show measurable exchange rates in the free toxin, remain unexchanged up to the longest incubation time, i.e., 24 h, in the Mα1–toxin complex (Table I). Therefore, only lower limits to their protection factors could be calculated. These limits equal 92 for N5 and 100 for K15. Two additional amides show significant protection factors in the Mα1–toxin complex (Table I), i.e., those of T13 ($\tau_1 = 46$) and K58 ($\tau_1 = 58$). Lastly, no conclusion can be drawn as to the protection of the amides of I35 and I36: only a lower limit of 5 could be obtained for their protection factors. Thus, four amides are clearly protected by Mα1: three of them (N5, T13, K15) are found in loop 1, and the last amide (K58) is found in the C-terminal part of the polypeptide chain (Figure 4a). K58 is close to the region defined by the three other residues: its side chain makes van der Waals contacts with amino acids of the upper part of loop 1.

Table I also displays several amides which are clearly not significantly protected by the antibody. First, the exchange

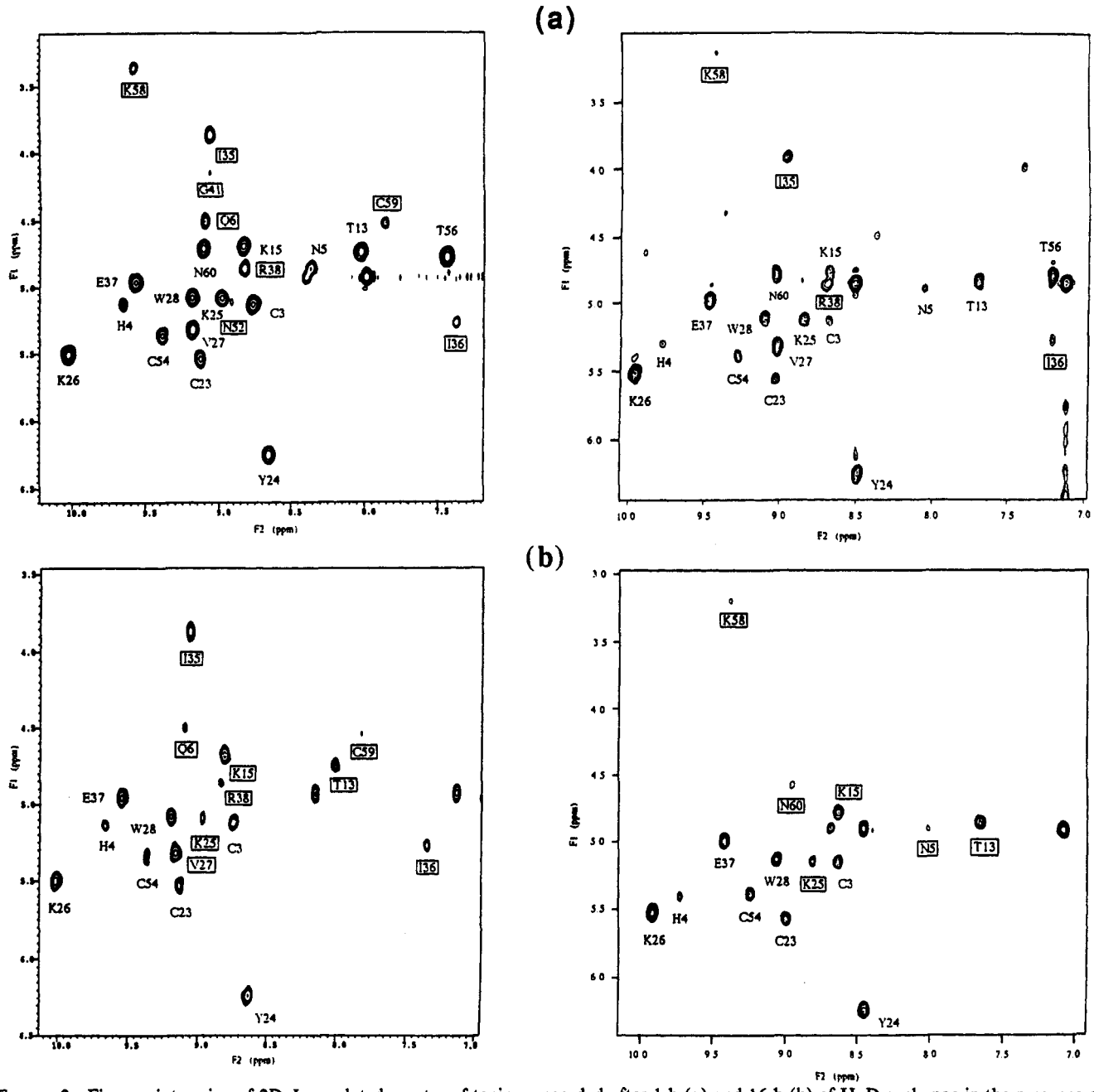

FIGURE 2: Fingerprint region of 2D J-correlated spectra of toxin α recorded after 1 h (a) and 16 h (b) of H–D exchange in the presence of Mα2,3 (left) or Mα1 (right). The cross peaks labeled by boxed names are not observed in the spectrum of the free toxin recorded at the same exchange time; these cross peaks result from antibody binding.

of the amides of Q6 and R38 is not slowed upon antibody binding. Thus, the contact region between loop 1 and loop 2 (Figure 4a) is not involved in the binding to Mα1. Second, the amide exchange of K25, V27, and W28 is not significantly perturbed by the binding. Thus, the central part of loop 2 (Figure 4a) does not contribute to the epitope. Finally, since the amides of T56, C59, and N60 are not protected by Mα1, most of the C-terminal chain (Figure 4a) is not involved in the interaction.

H–D Exchange in Mα2,3-Bound Toxin. In the Mα2,3-toxin complex, eight amides show a protection factor larger than 10 (Table I). They correspond to Q6 and K15 in loop 1; K25, V27, I35, I36, and R38 in loop 2; and C59 in the C-terminal part of the polypeptide chain (Figure 4b). Interestingly, none of these amides remains totally unexchanged during 24 h. For three additional amides, i.e., W28, G41, and N52, only lower limits of the protection factors could be obtained, equal to 3, 7, and 2, respectively (Table I). Thus, no conclusion can be given regarding their protection. However, the proximity of highly protected protons around the amide of W28 allows us to suggest that this amide belongs to the epitope. Figure 4b shows that most protected amides are located in the central part of loop 2. Loop 1 and the C-terminal chain also contain protected amides corresponding to Q6, K15, and C59. As illustrated in Figure 4b, the amide of Q6 is located at the limit of the β-strand of loop 1 which forms a short β-sheet with a β-strand of loop 2; it makes van der Waals contacts with R38 in loop 2. In contrast, K15 and C59 are not involved in direct interactions with loop 2 and are farther in space from the other residues.

Table I displays protection factors ranging from 1 to 10 for the amides of N5 and T13 in loop 1 and for the amides of T56, K58, and N60 in the C-terminal chain. Thus, the central part of loop 1 (Figure 4b) does not contribute to the epitope.

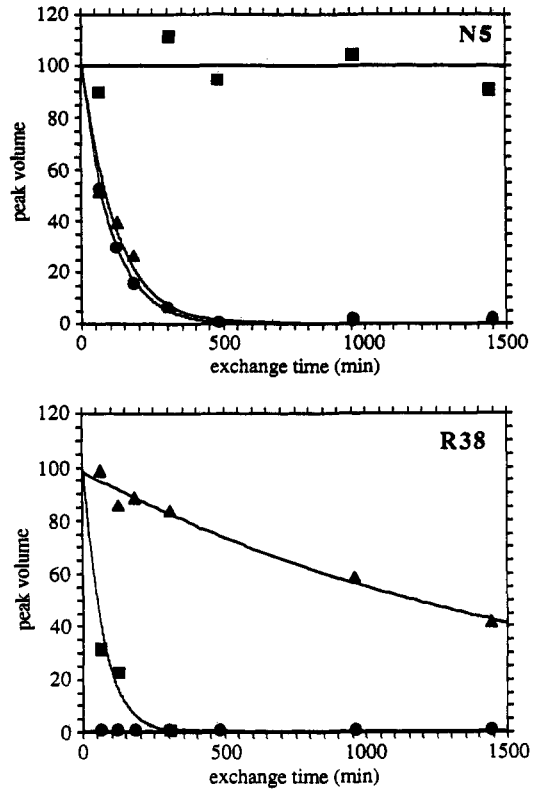

FIGURE 3: H–D exchange kinetics for the amide protons of N5 and R38 in free toxin α (●), in Mα1-bound toxin α (■), and in Mα2,3-bound toxin α (▲). The normalized volumes for the COSY (NH–C$^{\alpha}$H) cross peaks are plotted as a function of the H–D exchange time.

Similarly, most of the C-terminal chain (Figure 4b) is not involved in the interaction.

DISCUSSION

Interpretation of the Exchange Data. The exchange experiments were performed under well-defined pH and temperature conditions. A pH close to 7 was optimal for the binding of toxin α to the antibodies. The temperature was relatively low, so that the H–D exchanges of a substantial number of amides were sufficiently slow to be followed by the NMR approach used here. Furthermore, we have chosen a pH close to that of physiological conditions and a temperature which is more than 50 °C below the midpoint of thermal denaturation of the toxin, in order to minimize the contribution of cooperative unfolding to the exchange kinetics (Woodward et al., 1982; Tüchsen & Woodward, 1987). As a consequence, the H–D exchange experiments are expected to reflect the properties of the folded state, and the mechanisms of exchange in both the free and the bound toxin should involve only a low activation energy process (Woodward et al., 1982). Several models for this process have been proposed, including the local unfolding model (Englander, 1975; Englander et al., 1980), the mobile defect penetration model (Lumry & Rosenberg, 1975), the expansile cavity model (Richards, 1979), and the multistates model (Wagner & Wüthrich, 1979a,b). These models have been discussed in several reviews and papers (Woodward & Hilton, 1979; Banksdale & Rosenberg, 1982; Woodward et al., 1982; Englander & Kallenbach, 1984; Tüchsen & Woodward, 1985a,b, 1987). It is now widely agreed that the two main factors which influence hydrogen exchange are solvent proximity, i.e., proximity of the amide nitrogen to the surface of the protein, and hydrogen bonding in the main chain, particularly in α-helices and

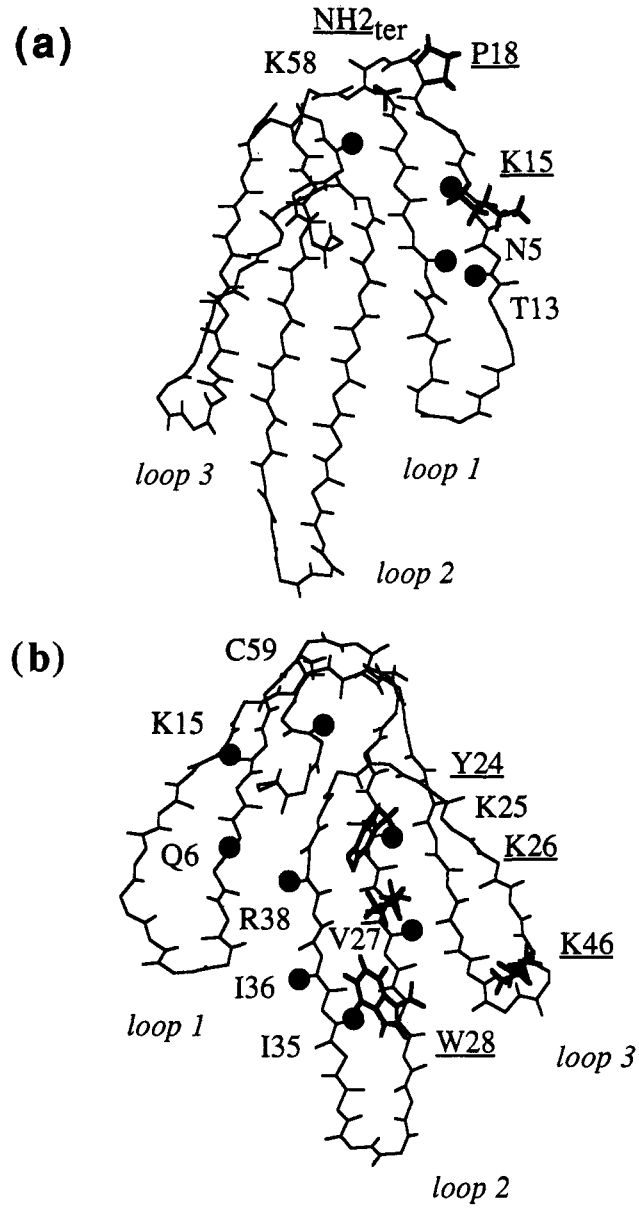

FIGURE 4: Spatial distribution of the amides (black spheres) protected from hydrogen exchange by the interaction with Mα1 (a) and Mα2,3 (b). The side chains displayed in bold have been described as being critical for the binding to the antibody on the basis of chemical modification experiments [reviewed in Ménez et al. (1992)]. The average backbone structure of toxin α is from Zinn-Justin et al. (1992). All the amide protons and carbonyl oxygens of the polypeptide chain are represented. Hydrogen bond acceptors are the main-chain carbonyl oxygens of the opposite strand of the β-sheet structure for the protected amides corresponding to residues N5 and K15 in panel a and residues K15, K25, V27, and I35 in panel b. They have not been clearly identified for the other protected amides (Zinn-Justin et al., 1992). Notice that the orientation of toxin α is different in (a) and (b).

β-sheets. It must be stressed that these two factors are sensitive to the fluctuation of the structure, which enables buried hydrogens to make contact with solvent molecules or which may involve a transient breaking of hydrogen bonds.

In our case, no increase of H–D exchange rates has been observed in the Mα1–toxin and Mα2,3–toxin complexes. This argues for the preservation of the β-sheet structure in toxin α and thus for the absence of substantial conformational changes in the three-dimensional structure of toxin α upon binding to the antibodies. Under these conditions, each of the above two factors predicts that labile protons at the surface

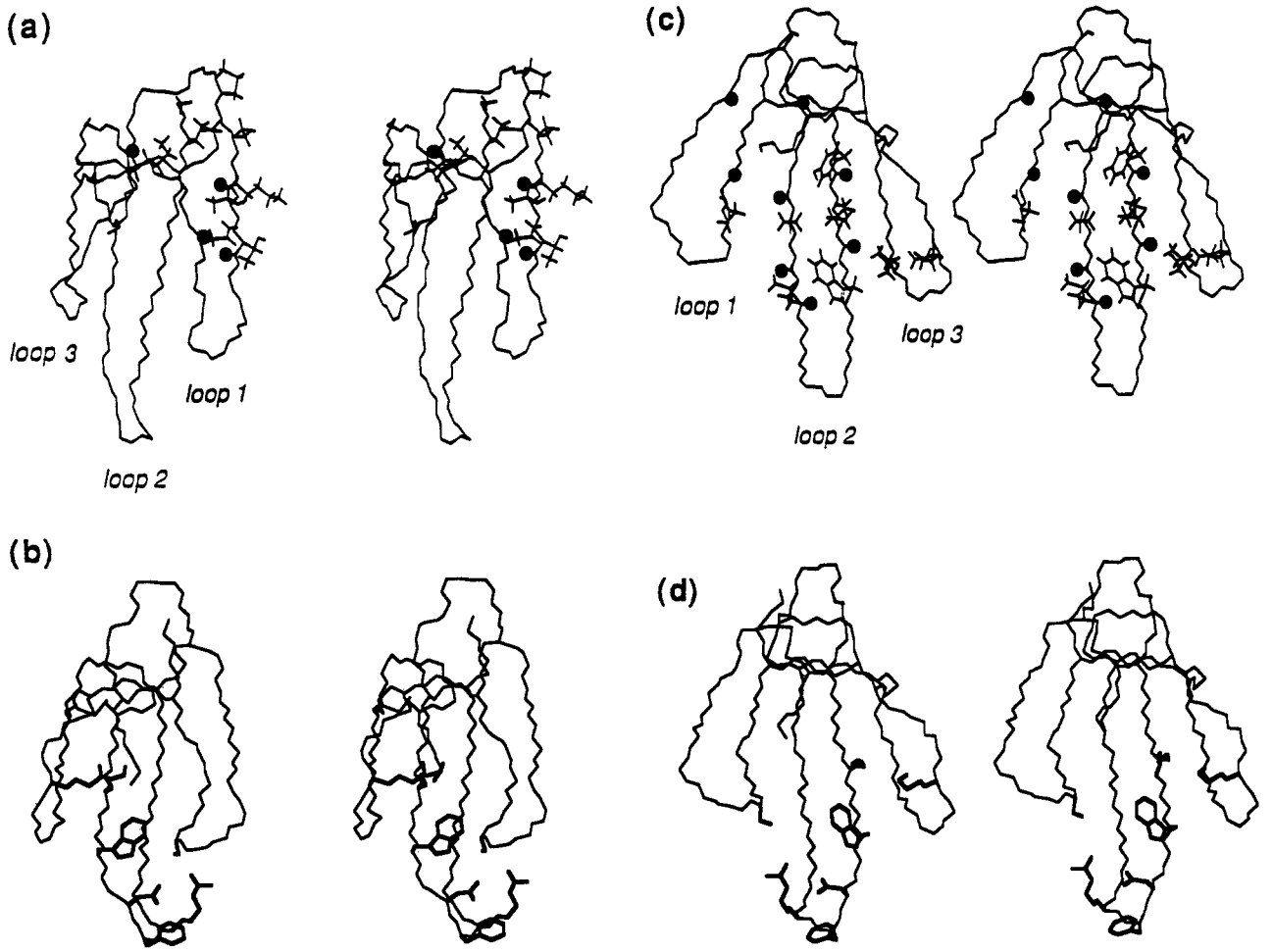

FIGURE 5: Proposed antigenic sites of toxin α: interactions with Mα1 (a) and Mα2,3 (c). The backbone, the disulfide bridges, and the side chains involved in the interaction with the antibody are represented. By comparison, panels b and d display the side chains involved in the toxic site of short-chain curaremimetic toxins and identified by Pillet et al. (1993) on the basis of experiments on erabutoxin a from *Laticauda semifasciata*. In vertically paired panels (a,b and c,d), the structures of toxin α and erabutoxin a are represented with the same orientation. The structure of toxin α is from Zinn-Justin et al. (1992). The coordinates of erabutoxin a (Corfield et al., 1989) are from the Protein Data Bank, Brookhaven National Laboratory (Reference: 5EBX).

interacting with the antibody should exhibit a slow exchange. However, a long-distance effect of antibody binding on the flexibility of the toxin may cause a decrease of the exchange rate for residues outside the epitope. This can be recognized in two combined ways. The detailed analysis of the topology of residues assigned to the epitope by exchange labeling must yield a contiguous surface, and the size of the epitope must be comparable to that of the crystallographically determined antigenic sites (Mayne et al., 1992).

Mα1–Toxin α Interaction Site. The antigenic site recognized by Mα1 appears to be centered on loop 1 (Figure 4a), whereas loop 2 does not seem to be involved in the interaction (Table I).

In order to define more precisely the limits of the epitope in loop 1, the role of the seven potentially observable amides of loop 1 has been examined (Figure 1). The amides of C3 and H4 do not exchange in either the free or the bound toxin, whereas the amides of E2 and Q10 fully exchange in 1 h in both the free and bound toxins. Thus, it is difficult to assess the role of residues located at the top and at the edge of loop 1. It can only be concluded that the two regions corresponding to the amides of E2 (top) and Q10 (edge) are not totally inaccessible to the solvent in the complex.

Chemical modification experiments (Boulain et al., 1982) have suggested that the NH_2 terminus and the side chain of K15 are critical for the binding to Mα1. Figure 4a shows that the region defined by the amides N5, T13, and K15 clearly contains the side chain of K15 and that the amide of K58 is close to the NH_2 terminus. An additional residue, i.e., P18, has been pointed out as being important for the interaction on the basis of comparison of sequences of homologous toxins (Boulain et al., 1982). This residue is located at the top of loop 1, in a region where our method cannot give precise information. Furthermore, the present study suggests that loops 2 and 3 are not involved in the binding to Mα1. Consistently, it has been found that the Mα1–toxin interaction was not affected by chemical modifications at positions Y24, K26, and W28 in loop 2 and K46 and K50 in loop 3 (Boulain et al., 1982; Ménez et al., 1992).

Examination of the backbone region defined on the basis of the NMR work suggests that the surface recognized by Mα1 consists essentially of a group of side chains located in the upper area of loop 1 and in the C-terminal part in contact with this area (Figure 5a). This group comprises the side chains of N5, T13, and K15, which are oriented as K15, the side chains of E2, T14, T16, P18, and K58, which are oriented as P18, and the NH_2 terminus (Figure 5a). Altogether, these side chains form a continuous solvent-accessible surface, which covers part of both sides of loop 1. The summed water-accessible surface (Lee & Richards, 1971) of the side chains corresponds to 750 Å^2. This value is consistent with the surfaces of the crystallographically determined epitopes in

antibody complexes with macromolecular antigens (Amit et al., 1986; Sheriff et al., 1987; Colman et al., 1987, 1989; Padlan et al., 1989; Bentley et al., 1990; Tulip et al., 1992). However, it must be noticed that not all of the proposed side chains are necessarily involved in a direct interaction with the antibody.

Mα2,3–Toxin α Interaction Site. The epitope recognized by Mα2,3 is centered on loop 2 (Figure 4b). Loop 1 and the C-terminal chain also contain protected amides which correspond to Q6, K15, and C59. Among these residues, Q6 makes contact with loop 2. Conversely, K15 and C59 are not involved in direct interactions with loop 2 and are farther in space from the other residues. The high protection factors of K15 and C59 may be due to a change in the flexibility of the toxin upon binding to Mα2,3. In fact, in our previous work (Zinn-Justin et al., 1992), C59 and K15 have been found to belong to the most highly constrained region of toxin α, i.e., the disulfide region. C59 is directly involved in a disulfide. K15 is the residue opposite C3 in the double-stranded β-sheet of loop 1; thus it shares two hydrogen bonds with C3, which is involved in a disulfide. As described by Mayne et al. (1992), a reduced flexibility of the epitope due to antibody binding may spread into adjacent highly stable parts of the structure, i.e., in our case, the disulfide region, and thus decrease the amide exchange rates of K15 and C59. It is more difficult to discuss the role of loop 3 in the binding. Indeed, only five amides of loop 3 are potentially observable in the complex. Four of them, i.e., the amides of T44, I49, K50, and L51, are not observed after 1 h of exchange in the bound toxin. This simply means that the central part of loop 3 is not totally inaccessible to the solvent due to the antibody. The fifth observable amide in loop 3 corresponds to N52. Only a lower limit of 2 characterizes the protection factor of this residue, for which no conclusion can be drawn.

Chemical modification experiments (Trémeau et al., 1986) have indicated that the side chains of Y24, K26, and W28 in loop 2 and K46 in loop 3 are critical for the binding to Mα2,3. All these side chains are oriented toward the concave side of the toxin (Figure 4b). Thus, the biochemical results indicate the side of the β-sheet of loop 2 which is involved in the interaction with the antibody: the binding site should be centered on the concave side of loop 2. It has also been shown that the Mα2,3–toxin interaction was not affected by chemical modifications at the NH_2 terminus and at K15 in loop 1 (Trémeau et al., 1986). This supports the proposition that the high protection factor of K15 is due to a change in the flexibility of the toxin upon binding to Mα2,3.

Thus, the surface of toxin α recognized by Mα2,3 consists essentially of a group of side chains which are located in the region mapped in this study (i.e., the central area of loop 2 and parts of loops 1 and 3 in contact with this area) and oriented toward the concave side of the toxin as indicated by the biochemical studies (Figure 5c). This group includes the side chains of Y24, K26, W28, I35, and E37 in the central part of loop 2, the side chain of Q7 in loop 1, which interacts with E37, the side chain of I49 in loop 3, which interacts with W28, and the side chain of K46, which interacts with I49. Figure 5c shows that these side chains form a continuous solvent-accessible surface. It should be noticed that not all of them necessarily interact directly with the antibody.

The resulting epitope includes one-half of the hydrophobic residues of toxin α (Zinn-Justin et al., 1992). Thus, hydrophobic interactions with the side chains of Y24, W28, I35, and I49 might be essential for the stabilization of the Mα2,3–toxin complex. Electrostatic interactions with the side chains of E37, K26, and K46 might also be involved in the binding.

The summed solvent-accessible surface (Lee & Richards, 1971) of the proposed side chains covers 550 $Å^2$. This value is somewhat smaller than the mean surface of the crystallographically determined epitopes in antibody complexes with macromolecular antigens (Amit et al., 1986; Sheriff et al., 1987; Colman et al., 1987, 1989; Padlan et al., 1989; Bentley et al., 1990; Tulip et al., 1992). However, no information has been obtained on the adjacent tip of loop 2 (Figure 1). Interestingly, if this region is assumed to be involved, at least partly, in the interaction, i.e., if some of the side chains of D30, H31, and R32, which are found on the concave side of the tip of loop 2, are involved in the binding, the resulting antigenic surface yields the usual value.

CONCLUSION

The measurement of proton exchange rates in two antibody–toxin α complexes allowed us to define a number of residues buried by the interaction with the antibodies and thus to obtain a general picture of the two epitopes. Eight side chains are proposed to participate in the epitope of each complex. These side chains belong to residues that are widely spread in the sequence but are brought together in space as a result of the protein folding. The resulting antigenic sites are centered on loop 1 (Mα1) and loop 2 (Mα2,3) of toxin α, respectively. They may be compared to the toxic site of toxin α as defined by various biochemical evidence.

Several experiments, based on measurements of the binding affinity of toxin α analogs for the nicotinic acetylcholine receptor, have shown that the toxic site of short-chain curaremimetic toxins is essentially located in loops 2 and 3, with the side chains of critical residues pointing toward the concave side of the molecule [reviewed in Endo and Tamiya (1987, 1991) and Pillet et al. (1993); see Figure 5b,d]. Thus, the epitopes recognized by Mα1 and Mα2,3 are located differently with respect to the toxic site (Figure 5). This appears to be related to the fact that Mα1 and Mα2,3 neutralize the toxin in two different ways.

Mα1 has been shown to accelerate the dissociation of the toxin–receptor complex (Boulain & Ménez, 1982). Our work shows that the binding site of Mα1 is distinct from the presumed toxic site (Figure 5a,b). Thus, the model of Boulain et al. (Boulain et al., 1982; Boulain & Ménez, 1982), in which Mα1 binds to the receptor-bound toxin, forming a transient ternary complex that destabilizes the toxin–receptor complex, finds here a structural support. Furthermore, the present NMR data indicate that no relevant changes occur in the three-dimensional structure of toxin α upon binding to Mα1. Thus, if conformational changes due to Mα1 binding are the reason for the accelerated dissociation of the toxin–receptor complex, these changes must be subtle. One may notice that different amides located in the central part of loop 2, i.e., those of K25, I35, and I36, show protection factors between 5 and 10. Although these values are difficult to interpret, the proximity of three low-protected amides in the three-dimensional structure of toxin α seems to indicate that the central part of loop 2 undergoes a change of flexibility upon binding to Mα1.

Interestingly, Mα2,3 has no effect on the toxin–receptor complex (our unpublished results). Moreover, the present work shows that the binding site of Mα2,3 in toxin α is centered on the concave face of loop 2 (Figure 5c): contrary to the Mα1 epitope, the Mα2,3 epitope covers most of the presumed toxic site of short-chain curaremimetic toxins (Figure 5d). Thus, the Mα2,3 neutralization process is clearly based on mutual exclusion of Mα2,3 and the receptor at the surface of

toxin α. It should be stressed that amino acids of the concave side of loop 2 are highly conserved in short-chain curaremimetic toxins. This finding is consistent with the fact that Mα2,3 neutralizes all tested short-chain curaremimetic toxins (Trémeau et al., 1986).

REFERENCES

Amit, A. G., Mariuzza, R. A., Phillips, S. E. V., & Poljak, R. J. (1986) *Science 233*, 747–753.

Aue, W. P., Bartholdi, E., & Ernst, R. R. (1976) *J. Chem. Phys. 64*, 2229–2246.

Banksdale, A. D., & Rosenberg, A. (1982) in *Methods of Biochemical Analysis* (Glick, D., Ed.) Vol. 28, pp 1–113.

Benjamin, D. C., Berzofsky, J. A., East, I. J., Gurd, F. R. N., Hannum, C., Leach, S. J., Margoliash, E., Michael, J. G., Miller, A., Prager, E. M., Reichlin, M., Sercarz, E. E., Smith-Gill, S. J., Todd, P. E., & Wilson, A. C. (1984) *Annu. Rev. Immunol. 2*, 67–101.

Bentley, G. A., Boulot, G., Riottot, M. M., & Poljak, R. J. (1990) *Nature 348*, 254–257.

Berkofsky, J. A. (1985) *Science 229*, 932–940.

Boulain, J.-C., & Ménez, A. (1982) *Science 217*, 732–733.

Boulain, J.-C., Ménez, A., Couderc, J., Faure, G., Liacopoulos, P., & Fromageot, P. (1982) *Biochemistry 21*, 2910–2915.

Brandt, P., & Woodward, C. K. (1987) *Biochemistry 26*, 3156–3162.

Burnens, A., Demotz, S., Corradin, G., Binz, H., & Bosshard, H. R. (1987) *Science 235*, 780–783.

Collawn, J. F., Wallace, C. J. A., Proudfoot, A. E. I., & Paterson, Y. (1988) *J. Biol. Chem. 263*, 8625–8634.

Colman, P. M., Laver, W. G., Varghese, J. N., Baker, A. T., Tulloch, P. A., Air, G. M., & Webster, R. G. (1987) *Nature 326*, 358–363.

Colman, P. M., Tulip, W. R., Varghese, J. N., Tulloch, P. A., Baker, A. T., Laver, W. G., Air, G. M., & Webster, R. G. (1989) *Philos. Trans. R. Soc. London, B 323*, 511–518.

Cooper, H. M., Jemmerson, R., Hunt, D. F., Griffin, P. R., Yates, J. R., III, Shabanowitz, J., Zhu, N.-Z., & Paterson, Y. (1987) *J. Biol. Chem. 262*, 11591–11597.

Davies, D. R., Padlan, E. A., & Sheriff, S. (1990) *Annu. Rev. Biochem. 59*, 439–473.

Eaker, D., & Porath, J. (1968) *Proc. Plenary Sess., Int. Congr. Biochem., 7th, 1967*, Column VIII-3, Abstr. III, p 499.

Endo, T., & Tamiya, N. (1987) *Pharmacol. Ther. 34*, 403–451.

Endo, T., & Tamiya, N. (1991) in *Snake Toxins* (Harvey, A. L., Ed.) pp 165–222, Pergamon Press, New York.

Englander, S. W. (1975) *Ann. N.Y. Acad. Sci. 244*, 10–27.

Englander, S. W., & Kallenbach, N. (1984) *Q. Rev. Biophys. 16*, 521–655.

Englander, S. W., Calhoun, D., Englander, J. J., Kallenbach, N., Liem, R., Malin, R., Mandal, C., & Rogero, J. (1980) *Biophys. J. 32*, 577–589.

Fryklund, L., & Eaker, D. (1975) *Biochemistry 14*, 2865–2871.

Jemmerson, R., & Margoliash, E. (1979) *J. Biol. Chem. 254*, 12706–12716.

Jemmerson, R., & Margoliash, E. (1981) *Methods Enzymol. 74*, 244–262.

Jemmerson, R., & Paterson, Y. (1986a) *Science 232*, 1001–1004.

Jemmerson, R., & Paterson, Y. (1986b) *Biotechniques 4*, 18–31.

Köhler, G., & Milstein, C. (1975) *Nature 256*, 495–497.

Lee, B., & Richards, F. M. (1971) *J. Mol. Biol. 55*, 379–400.

Lumry, R., & Rosenberg, A. (1975) *Colloq. Int. CNRS 246*, 55–63.

Mayne, L., Paterson, Y., Cerasoli, D., & Englander, S. W. (1992) *Biochemistry 31*, 10678–10685.

Ménez, A., Pillet, L., Léonetti, M., Bontems, F., & Maillère, B. (1992) in *Snake Toxins as Antigens: Structure of Antigens*, pp 293–320, Thomas Telford Ltd., London.

Nagayama, K., Kumar, A., Wüthrich, K., & Ernst, R. R. (1980) *J. Magn. Reson. 40*, 321–334.

Padlan, E. A., Silverton, E. W., Sheriff, S., Cohen, G. H., Smith-Gill, S. J., & Davies, D. R. (1989) *Proc. Natl. Acad. Sci. U.S.A. 86*, 5938–5942.

Paterson, Y. (1992) *Nature 356*, 456–457.

Paterson, Y., Englander, S. W., & Röder, H. (1990) *Science 249*, 755–759.

Pillet, L. (1991) Thèse de Doctorat, Université Paris XI.

Pillet, L., Trémeau, O., Ducancel, F., Drevet, P., Zinn-Justin, S., Pinkasfeld, S., Boulain, J.-C., & Ménez, A. (1993) *J. Biol. Chem. 268*, 909–916.

Richards, F. M. (1979) *Carlsberg Res. Commun. 44*, 47–63.

Sheriff, S., Silverton, E. W., Padlan, E. A., Cohen, G. H., Smith-Gill, S. J., Finzel, B. C., & Davies, D. R. (1987) *Proc. Natl. Acad. Sci. U.S.A. 84*, 8075–8079.

Trémeau, O., Boulain, J.-C., Couderc, J., Fromageot, P., & Ménez, A. (1986) *FEBS Lett. 208*, 236–240.

Tüchsen, E., & Woodward, C. (1985a) *J. Mol. Biol. 185*, 405–419.

Tüchsen, E., & Woodward, C. (1985b) *J. Mol. Biol. 185*, 421–430.

Tüchsen, E., & Woodward, C. (1987) *J. Mol. Biol. 193*, 793–802.

Tulip, W. R., Varghese, J. N., Laver, W. G., Webster, R. G., & Colman, P. M. (1992) *J. Mol. Biol. 227*, 122–148.

Urbanski, G. J., & Margoliash, J. (1977) *J. Immunol. 118*, 1170–1180.

Wagner, G., & Wüthrich, K. (1979a) *J. Mol. Biol. 130*, 31–37.

Wagner, G., & Wüthrich, K. (1979b) *J. Mol. Biol. 134*, 75–94.

Werner, M. H., & Wemmer, D. E. (1992) *J. Mol. Biol. 225*, 873–889.

Woodward, C. K., & Hilton, B. D. (1979) *Annu. Rev. Biophys. Bioeng. 8*, 99–127.

Woodward, C. K., Simon, I., & Tüchsen, E. (1982) *Mol. Cell. Biochem. 48*, 135–160.

Zinn-Justin, S., Roumestand, C., Gilquin, B., Bontems, F., Ménez, A., & Toma, F. (1992) *Biochemistry 31*, 11335–11347.